HHS Public Access

Author manuscript

Bone. Author manuscript; available in PMC 2022 July 01.

Published in final edited form as:

Bone. 2021 July ; 148: 115905. doi:10.1016/j.bone.2021.115905.

FOXO1 expression in chondrocytes modulates cartilage production and removal in fracture healing

Zhenjiang Ding[a,b,*], **Min Qiu**[b,c,*], **Mohammed A. Alharbi**[b,d,*], **Tiffany Huang**[b], **Xiyan Pei**[b,e], **Tatyana N. Milovanova**[b], **Hongli Jiao**[b], **Chanyi Lu**[b], **Min Liu**[b], **Ling Qin**[f], **Dana T. Graves**[b]

[a]Department of Pediatric Dentistry, School and Hospital of Stomatology, China Medical University, Liaoning Provincial Key Laboratory of Oral Diseases, Shenyang, China

[b]Department of Periodontics, School of Dental Medicine, University of Pennsylvania, Philadelphia, PA, USA

[c]Department of Orthopaedic Surgery, Shengjing Hospital, China Medical University, Shenyang, China

[d]Department of Endodontics, Faculty of Dentistry, King Abdulaziz University, Jeddah, KSA

[e]First Clinical Division, Peking University School and Hospital of Stomatology & National Clinical Research Center for Oral Diseases & National Engineering Laboratory for Digital and Material Technology of Stomatology & Beijing Key Laboratory of Digital Stomatology, China

[f]McKay Orthopaedic Research Laboratory, Perelman School of Medicine, University of Pennsylvania, Philadelphia, PA, USA

Abstract

Fracture healing is a multistage process characterized by inflammation, cartilage formation, bone deposition, and remodeling. Chondrocytes are important in producing cartilage that forms the initial anlagen for the hard callus needed to stabilize the fracture site. We examined the role of FOXO1 by selective ablation of FOXO1 in chondrocytes mediated by Col2α1 driven Cre recombinase. Experimental mice with lineage-specific FOXO1 deletion ($Col2\alpha1Cre^{+}FOXO1^{L/L}$) and negative control littermates ($Col2\alpha1Cre^{-}FOXO1^{L/L}$) were used for in vivo, closed fracture studies. Unexpectedly, we found that in the early phases of fracture healing, FOXO1 deletion significantly increased the amount of cartilage formed, whereas, in later periods, FOXO1 deletion led to a greater loss of cartilage. FOXO1 was functionally important as its deletion in chondrocytes led to diminished bone formation on day 22. Mechanistically, the early effects of FOXO1 deletion

Corresponding author: Dana T. Graves, DDS, DMSc, Phone: 215.898.9068, dtgraves@upenn.edu (D.T. Graves).

*These authors contributed equally.

Authors' roles: The overall study was conceived by DG; experiments were designed by - DG, ZD, and MQ; experiments were performed by - ZD, MQ, TH, TM, HJ, CL, and MA; data was interpreted by - DG, ZD, MQ, TH, LQ and TM; and the manuscript was written or edited by DG, LQ, ZD, and MA.

Declaration of competing interest

The authors declare no conflicts of interest.

were linked to increased proliferation of chondrocytes through enhanced expression of cell cycle genes that promote proliferation and reduced expression of those that inhibit it and increased expression of cartilage matrix genes. At later time points experimental mice with FOXO1 deletion had greater loss of cartilage, enhanced formation of osteoclasts, increased IL-6 and reduced numbers of M2 macrophages. These results identify FOXO1 as a transcription factor that regulates chondrocyte behavior by limiting the early expansion of cartilage and preventing rapid cartilage loss at later phases.

Keywords

Fracture; Healing; Chondrocyte; Cartilage; Osteoclast; Inflammation

1. Introduction

Fracture healing is a complex process in which the repair is accomplished by both intramembranous bone formation and the fracture callus stabilized by endochondral ossification (1–3). After the formation of a hematoma, the area of the fracture is infiltrated by skeletal stem cells, a subset of mesenchymal stem cells. Skeletal stem cells give rise to chondrocytes that form cartilage and play a key role in resolving inflammation that occurs early in the repair process (4, 5). In addition to producing cartilage matrix, it is recently appreciated that chondrocytes influence events such as angiogenesis (6). Chondrocytes rapidly undergo a series of cellular events including early proliferation, production of matrix, hypertrophy and eventual apoptosis or differentiation into osteoblasts (7, 8).

Macrophages contribute to fracture healing and exist in multiple forms with the best characterized being M1 and M2 macrophages (9). M1 macrophages exhibit a pro-inflammatory phenotype and are associated with expression of inflammatory cytokines such as tumor necrosis factor- α (TNF- α), interleukin- 1β (IL- 1β), interleukin- 6 (IL- 6), and monocyte chemotactic protein- 1 (MCP- 1) (10, 11). M2 macrophages produce anti-inflammatory cytokines and growth factors and are linked to the resolution of inflammation and healing events (10, 11).

FOXO transcription factors consist of four different proteins, FOXO1, FOXO3, FOXO4, and FOXO6. FOXO1, FOXO3, and FOXO4 are ubiquitously expressed, whereas FOXO6 expression is largely restricted to the brain (12). In bone, FOXO1 modulates osteoblast differentiation by interacting with other signaling pathways, including Runx2 and Wnt/b-catenin (13–15). FOXO1 expression is important in chondrocytes and reduces osteoarthritis by preserving chondrocytes and by inducing expression of lubricin that protects cartilage from wear (16). We have demonstrated that FOXO1 significantly contributes to normal fracture healing by regulating chondrocyte expression of VEGF that promotes angiogenesis during the transition from cartilage to bone (6). In contrast, FOXO1 is dysregulated in diabetic fracture healing and induces chondrocytes to produce RANKL leading to premature removal of cartilage (17). Recent evidence suggests that the latter is due to the impact of high glucose on FOXO1 interaction with the RANKL promoter to stimulate osteoclast

formation and the accelerated loss of cartilage, leaving a reduced template for bone formation that diminishes mechanical strength (18, 19).

Although the impact of FOXO1 in diabetic fracture healing has been well studied (18–21), less is known about the impact of FOXO1 in normoglycemic conditions. Thus, we sought to investigate how FOXO1 regulates chondrocytes to contribute to normal fracture healing and identify responsible mechanisms. Unexpectedly, we found that in the early phases of fracture healing, FOXO1 deletion significantly increased the amount of cartilage formed, whereas, in later periods, FOXO1 deletion greatly accelerated the loss of cartilage. Thus, FOXO1 regulates chondrocyte activity that restrains cartilage production initially and helps to preserve cartilage in later phases of healing.

2. Material and Methods

2.1 Animals and fracture induction

All animal studies were carried out with approval from the University of Pennsylvania Institutional Animal Care and Use Committee (IACUC), and mice were monitored daily by University Laboratory Animal Services (ULAR). Experiments were performed on experimental Col2α1Cre^{+}FOXO1$^{L/L}$ mice and littermate controls, Col2α1Cre^{-}FOXO1$^{L/L}$ mice. A modified allele of FOXO1 was used to generate a null allele after Cre mediated recombination where exon 2 is flanked by loxP sites (FOXO1^{L}). Then a transgene expressing Cre recombinase from the collagen2α1 promoter B6;SJL-Tg(Col2a1-cre)1Bhr/J was used to generate the chondrocytes with null alleles of FOXO1. Following the standard breeding schemes, Col2α1Cre$^{+/-}$FOXO1$^{L/L}$ crossed with Col2αCre $^{-/-}$FOXO1$^{L/L}$(Col2α1Cre^{-}FOXO1$^{L/L}$) to produce and experimental and control mice, which were directly compared in each litter (19). The background of these mice is largely C57B/6. Mice with a known genotype from each litter were randomly assigned to groups with a similar distribution of male and female mice for each. Two to five mice were housed per cage under standard conditions with 14-h light/10-h dark cycles. The presence of Cre recombinase and floxed FOXO1 was confirmed by PCR of genomic DNA prior to performing experiments and again at the time of euthanasia. Primers used for all PCR experiments are shown in Supplemental Table 1.

Closed-transverse fractures were performed on the femur of 12-15-week-old adult mice as described previously (21). The leg was scrubbed with 10% iodine and a 5-mm medial, parapatellar incision was made to expose the femoral condyle. A 30-gauge needle was used to drill a hole into the femoral medullary canal in the groove of the femoral condyle. A 0.01” stainless steel needle was inserted into the femoral canal to stabilize the fracture and was secured by insertion of a 30-gauge needle. The incision was closed with 5–0 resorbable sutures, and the fracture was induced using a 3-point impact bending device. The animal was allowed to move freely with unrestricted weight-bearing after recovery from anesthesia. Fractures that were not mid diaphyseal or that were grossly comminuted were excluded from the study. Extended release Buprenorphine (3.25 mg per kg) was given as analgesic immediately before the fracture induction and continued every 72 hours for 7 days. (B1637-100MG, Spectrum Chemical Manufacturing Corporation, California, USA)

2.2 Micro-Computed Tomography and Image Analysis:

Viva CT40 (Scanco Medical, Brüttisellen, Switzerland) was used to scan the specimens at 19μm voxel size. The following scan settings were used; 70 kVp, 114 mA, and 200ms integration time. A constrained, 3-D Gaussian filter (sigma=0.8, support=1) was used for noise reduction. A fixed global threshold was chosen that represented the transition in X-ray attenuation between mineralized and unmineralized tissue. Viva CT40 software was used for the 3D reconstructions. Segmentation and countering were achieved manually on a slice-by-slice basis.

Two calibrated examiners identified the beginning of the callus and the end point. The image data were analyzed using software provided by the system manufacturer in order to quantify the bone volume of the fracture callus. The first step in this analysis consisted of defining the outer boundary of the callus. This was done on every 12-μm-thick slice along the length of the callus. Bone volume (BV), tissue volume (TV) and total mineral density (TMD)were calculated from the sum of the areas by the slice thickness of each bone. BV/TV was calculated according to the BV and TV.

2.3 Histology and histomorphometric analysis

The femurs were carefully dissected, and the majority of the muscle tissue was removed. Samples were fixed for 24 hours in cold 4% paraformaldehyde and then decalcified for 5 weeks by incubation in 10% EDTA. To ensure that all the specimens were sectioned and imbedded in the center of the fracture line, radiographs were taken after euthanasia. The images were normalized (1:1 ratio with the actual specimen). The femurs were then aligned with the images taken with a dissecting microscope and sectioned into halves at the center of the fracture line with a sharp blade after decalcification and embedded in paraffin. Transverse paraffin sections were prepared as described and sections near the fracture site were examined (22). Since the fracture heals at different rates longitudinally, transverse sections near the fracture line provide a consistent view of the cellular events that occur during fracture healing (22), an approach we have taken in several publications (1, 19–21). Safranin O/Fast green–stained sections were assessed for cartilage area, hypertrophic area, transition area (chondro-osseous junction, as described (23) (Supplemental Fig. 1), bone area, and total callus by quantitative computer-assisted image analysis (NIS element software, Nikon, Japan). Multinucleated osteoclasts in the transition area were identified by tartrate-resistant acid phosphatase (TRAP) staining. Images of Safranin O/Fast green–stained and TRAP-stained sections were both captured under 10× and 20× objectives with a Nikon Eclipse 90i microscope (Nikon, Japan) and analyzed using a NIS Elements-AR software (Nikon, Japan).

2.4 Immunofluorescence

Paraffin sections were dewaxed, and antigen retrieval was performed at 95°C in 10 mmol/L citric acid, pH 6.0 for 20 min followed by nonspecific blocking with nonimmune serum matching the secondary antibody for 55 min. Single immunofluorescence staining was performed using primary antibody anti-IL-6 (ab7737, Abcam, Cambridge, MA, USA). Double immunofluorescence staining was then performed using the primary antibodies: anti-F4/80 (ab6640, Abcam, Cambridge, MA, USA) and anti-CD206 (ab64693, Abcam,

Cambridge, MA, USA), The appropriate isotype-matched IgG with the concentration adjusted to match the primary antibody was used as the negative control. Goat anti-rat (A10549, Thermo Fisher Scientific, Waltham, MA, USA) and goat anti-rabbit (NB7160, Novus Biologicals, Littleton, CO, USA) were used as secondary antibodies. Nuclei were counterstained with 4,6-diamidino-2-phenylindole (DAPI; ab104139, Abcam, Cambridge, MA, USA). A list of all antibodies used are shown in Supplemental Table 2. The region of interest, cartilage area and the transition zone were established by comparison of sections examined by immunofluorescence and adjacent sections stained with Safranin-O/Fast green as shown in Supplemental Figure 1. IL-6 expression was assessed in chondrocytes, which were identified by their location within cartilage. Images were captured under 10×, 20× and 40× objectives with a Nikon Eclipse 90i microscope (Nikon, Japan) and analyzed using a NIS Elements-AR software (Nikon, Japan). The mean number was calculated on six animals each group by the immunopositive cells divided by the area.

2.5 Cell culture and in vitro experiments

Primary costal chondrocytes were isolated from 2-4-day-old experimental Col2α1Cre $^{+}$FOXO1$^{L/L}$ and control Col2α1Cre^{-}FOXO1$^{L/L}$ mice as described before (24). Briefly, ribs were isolated, washed with PBS, incubated in pronase (Thermo Fisher Scientific, USA) for 45 min at 37°C to dissolve the soft tissue, and then they were washed with PBS followed by a 60-min-incubation in Collagenase D (11088858001, Roche, Waltham, MA, USA) to dissociate the hard tissue from the remaining soft tissues. Ribs were then incubated in collagenase D for 3–5 h at 37°C and released cells separated from debris with a 70-mm strainer and incubated in DMEM media supplemented with 10% FBS and 1% Antibiotic-Antimycotic (Anti-Anti; 15240062, Thermo Fisher Scientific, Waltham, MA, USA). ATDC5 chondrocytes were purchased from the American Type Culture Collection (ATCC; Manassas, VA, USA). Cells were cultured in 50% DMEM (11885084, Gibco, Gaithersburg, MD, USA) and 50% F12 with 5% FBS. All cell cultures were maintained in a 5% CO_2 humidified incubator at 37°C.

siRNA transfections were performed with cells at approximately 60% to 70% confluence in 6-well plates with 10nM siFOXO1 or matched scrambled control siRNA (Dharmacon, Lafayette, CO, USA) using GenMute transfection reagent (SL100568, SignaGen Laboratories, Rockville, MD, USA) following the manufacturer's instructions.

Serum starvation of primary chondrocytes and/or ATDC5 were performed in 0.5% FBS for 48 h and then stimulation with 10% FBS for 14 h. For growth curves, cells were cultured in a 96-well plate and counted with a hemocytometer with Trypan blue staining. Proliferation was measured by BrdU Assay with a kit from Cell Signaling Technology (6813S, Cell Signaling Technology, Danvers, USA) according to the manufacturer's protocol.

For mRNA analysis, RT-qPCR was performed with RNA extracted using an RNAqueous kit (AM1912, Ambion, Waltham, MA, USA). Reverse transcription was performed using High-Capacity RNA-to-cDNA Kit (4387406, Applied Biosystems, Foster City, CA, USA) and relative mRNA levels assessed using Fast SYBR Green Master Mix (4385612, Applied Biosystems, Foster City, CA, USA) on a StepOnePlus Real-time PCR system (4376600, Applied Biosystems, Foster City, CA, USA). Results were normalized with the

housekeeping gene L32 and relative mRNA calculated using the $\Delta\Delta$CT method. The sequences of all PCR primers were listed in Supplemental Table 1.

Expression at the protein level in vitro was measured by flow cytometry. Primary chondrocytes from experimental and control mice and ATDC5 chondrocytes were washed, fixed, and permeabilized using a kit (GAS003, Invitrogen, Waltham, MA, USA). Anti-Cyclin D1 (NBP2-34816AF488, Novus Biologicals, Littleton, CO, USA), anti-aggrecan (NB100-74350, Novus Biologicals, Littleton, CO, USA), anti-FOXO1 (NBP2-31376, Novus Biologicals, Littleton, CO, USA), and anti-IL-6 (NBP2-44953, Novus Biologicals, Littleton, CO, USA) were with/without conjugated with a fluorochrome for cell analysis and then compared to matched isotype control antibodies. For flow cytometry, the cells were incubated in the presence of 2.5 μg/ml fluorochrome-labeled antibody and examined by FACS analysis on LSR II (BD Biosciences, FACSDiva Software). The results were analyzed in FlowJo 10.7 version (Tree Star Inc. Ashland, OR, USA). Experiments were in triplicate and each experiment was performed three times with similar results.

2.6 Statistical analysis

The results of male and female mice from the same group were combined. When comparing multiple groups, ANOVA with Tukey's post hoc test was carried out in vitro and in vivo assays. When comparing two groups, two-tailed Student's t-test for unpaired samples was performed. Significance was set at $p < 0.05$. For in vitro assays, a minimum of three samples were examined per group and three independent experiments were carried out with similar results. For in vivo immunofluorescence, there was a minimum of six specimens per group.

3. Results

3.1 FOXO1 deletion in chondrocytes increases both cartilage formation and loss

Safranin O/Fast green staining was performed on histologic sections obtained from the fracture midline to assess cartilage, area of hypertrophic chondrocytes, the chondro-osseous junction consisting of mixed cartilage and bone (transition area) and callus size (Fig. 1A-D). On days 7 and 10, the callus size and cartilage area in the experimental Col2α1Cre $^{+}$FOXO1$^{L/L}$ mice were significantly larger than matched controls, but on days 13 and 16 this pattern was reversed, so that the control mice had larger calluses and cartilage area compared to the experimental group. Histomorphometry indicated that cartilage in the Col2α1Cre^{+}FOXO1$^{L/L}$ group was increased 308% on day 7 and 124% on day 10 compared to control littermates ($p < 0.05$). However, the cartilage area in the experimental group was reduced by 47% on day 13 and 80% on day 16 compared to the matched control ($p < 0.05$, Fig. 1E). The area of hypertrophic cartilage was initially higher in mice with deletion of FOXO1 in chondrocytes and later became significantly smaller in this group compared to the control group ($p < 0.05$, Fig. 1F). The area of the chondro-osseous junction (transition area), which reflects a region of the callus undergoing cartilage resorption and bone formation, was approximately 50% smaller on days 13 and 16 in the experimental mice versus control mice ($p < 0.05$, Fig. 1G). Changes in the overall fracture callus area in this time frame largely reflected the changes in the cartilage area. Col2α1Cre^{+}FOXO1$^{L/L}$ mice had a callus size that was 64% larger on day 7 and 46% on day 10 but were approximately

20–30% smaller on days 13 and 16 (p <0.05, Fig. 1H). On day 16 and 22 post-fracture, both bone volume and total callus volume in Cre^+ group with FOXO1 deletion were significant smaller when compared to the control group ($p < 0.05$, Table 1).Representative images are presented in supplemental Fig. 3. There was no statistically significant difference in the bone volume/ total volume between both groups. (Table 1)

A summary of the changes in the size of the callus, cartilage, transition zone and bone are shown in Supplemental Table 3. When histologic specimens from male and female mice were examined separately there was no trend suggesting a gender-based difference between them.

3.2 FOXO1 deletion in chondrocytes promotes cell proliferation and the expression of cartilage matrix genes.

In vitro studies were undertaken to assess the effect of FOXO1 deletion under defined conditions in primary chondrocytes from experimental and littermate control mice or by FOXO1 knockdown by RNAi in ATDC5 chondrocytes. Primary chondrocytes from mice with FOXO1 ablation increased in numbers at a higher rate than control chondrocytes ($p < 0.05$, Fig. 2A). By BrdU assay DNA synthesis in ATDC5 chondrocytes was 65% higher with FOXO1 knockdown compared with scrambled siRNA ($p < 0.05$, Fig. 2B). FOXO1 deletion or knockdown altered the level of cell cycle genes stimulated by 10% FBS, increasing Cyclin D1 by 92% in primary chondrocytes and by 49% in ATDC5 chondrocytes compared to matched controls ($p < 0.05$, Fig. 2C, D). Cyclin D1 protein levels measured by flow cytometry were significantly increased by FOXO1 ablation in primary chondrocytes and by FOXO1 knockdown in ATDC5 chondrocytes (Fig. 2E, F). In contrast, the inhibitory cell cycle factor, p27 was decreased by 39% in FOXO1-deleted primary chondrocytes and 24% in ATDC5 chondrocytes at the mRNA level ($p < 0.05$, Fig. 2G, H).

We next examined the FOXO1 regulation of key components of the cartilage matrix. FOXO1 ablation increased aggrecan core protein mRNA levels by 44% in primary chondrocytes and FOXO1 knockdown increased aggrecan by 334% in ATDC5 chondrocytes ($p < 0.05$, Fig. 2I, J). At the protein level, aggrecan was significantly increased by FOXO1 deletion in primary chondrocytes and ATDC5 chondrocytes with FOXO1 knockdown (Fig. 2K, L). Collagen Col10α1 exhibited similar changes with a 65% increase in primary chondrocytes with FOXO1 ablation and a 106% increase in ATDC5 chondrocytes with FOXO1 knockdown ($p < 0.05$, Fig. 2M, N). Control experiments determined that FOXO1 mRNA and protein levels were significantly reduced by 70–85% in both primary chondrocytes from experimental mice with FOXO1 ablation and ATDC5 chondrocytes with FOXO1 knockdown compared to matched controls (Fig. 2O-R). Cyclin D1, p27, IL-6, aggrecan and Col10α1 have strong FOXO1 consensus response elements as determined by JASPAR analysis (Supplemental Table 4).

3.3 FOXO1 deletion in chondrocytes increases osteoclast numbers

Since FOXO1 deletion after day 10 caused a rapid loss of cartilage, we determined whether there were differences in the level of osteoclasts. The number of $TRAP^+$ osteoclasts lining the cartilage surface was greater in fractures of mice with FOXO1-ablated chondrocytes The

magnification of the low power is 10x and the high power is 20x. Scale bars = 100 μm. (Fig. 3A). FOXO1 deletion in chondrocytes increased osteoclast numbers by 98% on day 13 and 53% on day 16 (Fig. 3C, D). In contrast, there was no difference in MMP13 expression in the experimental group with FOXO1 deleted in chondrocytes compared to the matched control group, suggesting that the greater loss of cartilage in the FOXO1-deleted group is not due to MMP13 (Suppl Fig 2).

To assess how FOXO1 expression in chondrocytes might affect the local environment to increase osteoclast numbers we examined the number of IL-6 immunopositive cells during the early phase of pronounced osteoclast formation. The region of interest, the cartilage area was established by comparison of sections examined by immunofluorescence and adjacent sections stained with Safranin O/Fast green (Fig. 4A). The specificity of immunostaining was determined by comparison of results with specific antibodies with matched control antibodies. The number of IL-6 immunopositive cells was increased by 127% in Col2α1Cre^{+}FOXO1$^{L/L}$ group when compared with Col2α1Cre^{-}FOXO1$^{L/L}$ ($p < 0.05$, Fig. 4B). The impact of FOXO1 deletion on IL-6 expression in vitro was consistent with in vivo results. FOXO1 deletion increased IL-6 mRNA level by 87% in primary chondrocytes with FOXO1 ablation and FOXO1 siRNA increased IL-6 by and 177% increase in ATDC5 chondrocytes compared to scrambled siRNA ($p < 0.05$, Fig. 4C, D). At the protein level, IL-6 was increased by 70–110% in primary chondrocytes with FOXO1 deletion or ATDC5 chondrocytes with FOXO1 knockdown ($p < 0.05$, Fig. 4E, F). Besides, we also detected the M2 macrophage formation by counting the number of F4/80^{+}CD206^{+} cells at the same time point (Fig. 4G). In contrast, the number of M2 macrophages was significantly less in the experimental mice with chondrocyte deletion of FOXO1 compared to the control group ($p < 0.05$, Fig. 4H).

4. Discussion

FOXO1 has a more dominant effect on chondrocytes than other FOXOs. We focused on FOXO1 based on previous reports that single FOXO1 deletion in chondrocytes as similar effects as triple FOXO1,3,4 deletions whereas single deletion of FOXO3 or FOXO4 has a relatively small effect (16, 25). Here, we assessed the role of chondrocytes in fracture healing in mice with lineage-specific deletion of FOXO1 in chondrocytes. The central importance of this study is the finding that FOXO1 plays an important role in the behavior of chondrocytes that has an impact on early cartilage formation and later cartilage removal and that FOXO1 in chondrocytes is needed for normal fracture healing as reflected by the reduced amount of bone formed at later time points in the experimental group.

Closed fracture was induced in experimental mice with lineage-specific FOXO1 deletion (Col2α1Cre^{+}FOXO1$^{L/L}$) and negative control littermates (Col2α1Cre^{-} FOXO1$^{L/L}$). However, in order to compare the function of FOXO1, the studies in our group haven't been carried out with normal animals before. It has been reported that the measurements of cartilage and bone composition can be accurately quantified by use of transverse sections (26). Since our goal was to measure these aspects of fracture healing in and its impact by FOXO1 deletion in chondrocytes we chose to use this approach, which we have used in previous publications (6, 18, 19). The results indicate that FOXO1 plays a key role in

maintaining homeostasis by regulating activity in chondrocytes to limit excessive cartilage formation in early fracture healing and maintaining cartilage mass at later phases. It is striking that despite the larger cartilage and total callus area on day 7 there was significantly less cartilage and smaller calluses on day 13 with lineage-specific FOXO1 ablation in chondrocytes. In contrast, deletion of FOXO1 in chondrocytes has little effect on bone development as unfractured bone has similar bone parameters in experimental (Col2α1Cre $^{+}$FOXO1$^{L/L}$) and matched littermates (Col2α1Cre^{-}FOXO1$^{L/L}$)(18)

We had previously demonstrated that the deletion of FOXO1 in chondrocytes reduced the premature removal of cartilage associated with endochondral bone formation at the later time of fracture healing (19). Thus, the transcription factor FOXO1 facilitates normal fracture healing by restraining the early expansion of cartilage and at later time points, to reduce rapid cartilage loss. However, FOXO1 plays a different role in diabetic fracture healing. FOXO1 induced gene expression is altered by conditions that are present in diabetes such as high levels of glucose or advanced glycation endproducts, which in turn has physiologic consequences that are detrimental (17, 18, 21). Thus, in diabetic fracture healing FOXO1 promotes cartilage removal whereas in normal fracture healing FOXO1 acts to limit it.

When FOXO1 was deleted there was both an increase in the number of chondrocytes and matrix production which likely contribute to the increase in cartilage detected. We examined two types of chondrocytes in vitro, primary chondrocytes, and the ATDC5 chondrocyte cell line with similar and consistent results obtained with both. FOXO1 deletion or knockdown increased cyclin D1 that promotes proliferation and reduced p27 that inhibits it. Moreover, reduced FOXO1 through ablation or RNAi increased Col10α1 and aggrecan core protein. Thus, FOXO1 restrains the over-production of cartilage by acting as a brake on chondrocyte proliferation and expression of matrix proteins. The impact of FOXO1 on chondrocyte proliferation is consistent with reports that FOXO1 inhibits the proliferation of osteoblasts and glomerular mesangial cells (27). Overexpression of FOXO1 can decrease the production of extracellular matrix in glomerular mesangial cells, and down-regulation of FOXO1 can cause increased production of extracellular matrix proteins in these cells in vitro (28, 29). There have been several published studies with ChIP assays showing FOXO1 interaction with promoter region of Cyclin D1 (30) and P27 in several cell lines (31–33) to regulate the cell proliferation.

FOXO1 deletion in chondrocytes led to accelerated loss of cartilage during endochondral bone formation in the callus. Previous studies report that MMP-13 plays an essential role in cartilage remodeling during fracture-induced endochondral bone formation (34, 35). We found that FOXO1 deletion did not change MMP13 expression in chondrocytes. However, FOXO1 deletion in chondrocytes did significantly increase the number of osteoclasts lining cartilage during the period of rapid cartilage removal. To account for the increased numbers of osteoclasts, we examined inflammatory changes. IL-6 expression in chondrocytes significantly increased in fractures in the experimental group *in vivo*. This change was supported by increased IL-6 mRNA and IL-6 protein levels when FOXO1 was deleted or knocked down in chondrocytes *in vitro* and is consistent with reports that chondrocytes

produce IL-6 (36). Furthermore, IL- 6 activity is closely associated with osteoclast formation in vitro and vivo (37, 38).

We examined another aspect of fracture healing that could account for an altered level of inflammation by assessing anti-inflammatory M2 macrophages that were double positive for F4/80 (pan macrophage marker) and CD206 (M2-like macrophage marker) (39, 40). It has previously been shown that increased numbers of $F4/80^{+}CD206^{+}$ double-immunopositive macrophages are beneficial for resolving inflammation and reducing osteoclastogenesis (40, 41). A reduction in M2 macrophages has been reported to cause persistent inflammation in surgical wounds (42). Consistent with these observations, we found significantly reduced numbers of $F4/80^{+}CD206^{+}$ macrophages in the experimental $Col2\alpha1Cre^{+}FOXO1^{L/L}$ group compared to the matched negative Cre^{-} control group. These results point to a reduction in anti-inflammatory M2-like macrophages in the experimental group (43). We attempted to measure M1 macrophages by double immunofluorescence as $F4/80^{+}iNOS^{+}$ or $CD68^{+}iNOS^{+}$ cells but could not obtain results with convincing specificity.

In conclusion, our results show that specific deletion of FOXO1 in chondrocytes modulates chondrocyte activity to increase early cartilage formation and at later time points, leads to greater loss of cartilage. We previously examined the effect of lineage-specific deletion of FOXO1 in chondrocytes and established that the loss of FOXO1 in chondrocytes significantly reduces bone volume at 35 days post-fracture but the cellular changes were not established (19). Thus, we propose that FOXO1 in chondrocytes in normal fracture healing helps in maintaining the normal progression of cartilage formation and removal in the healing fractures to facilitate the formation of a more robust hard callus.

Supplementary Material

Refer to Web version on PubMed Central for supplementary material.

Acknowledgments

This work was supported by NIH grants R01AR060055 and R01DE017732.

Literature Cited

1. Ai-Aql ZS, Alagl AS, Graves DT, Gerstenfeld LC, Einhorn TA. Molecular mechanisms controlling bone formation during fracture healing and distraction osteogenesis. J Dent Res. 2008;87(2):107–18. [PubMed: 18218835]
2. Chang J, Liu F, Lee M, Wu B, Ting K, Zara JN, et al. NF-kappaB inhibits osteogenic differentiation of mesenchymal stem cells by promoting beta-catenin degradation. Proc Natl Acad Sci U S A. 2013;110(23):9469–74. [PubMed: 23690607]
3. Hu DP, Ferro F, Yang F, Taylor AJ, Chang W, Miclau T, et al. Cartilage to bone transformation during fracture healing is coordinated by the invading vasculature and induction of the core pluripotency genes. Development. 2017;144(2):221–34. [PubMed: 28096214]
4. Marsell R, Einhorn TA. The biology of fracture healing. Injury.2011;42(6):551–5. [PubMed: 21489527]
5. Ko KI, Syverson AL, Kralik RM, Choi J, DerGarabedian BP, Chen C, et al. Diabetes-Induced NF-kappaB Dysregulation in Skeletal Stem Cells Prevents Resolution of Inflammation. Diabetes. 2019;68(11):2095–106. [PubMed: 31439641]

6. Zhang C, Feinberg D, Alharbi M, Ding Z, Lu C, O'Connor JP, et al. Chondrocytes Promote Vascularization in Fracture Healing Through a FOXO1-Dependent Mechanism. J Bone Miner Res. 2019;34(3):547–56. [PubMed: 30347467]
7. Singh A, Mehdi AA, Srivastava RN, Verma NS. Immunoregulation of bone remodelling. Int J Crit Illn Inj Sci. 2012;2(2):75–81. [PubMed: 22837895]
8. Wong SA, Rivera KO, Miclau T 3rd,, Alsberg E, Marcucio RS, Bahney CS Microenvironmental Regulation of Chondrocyte Plasticity in Endochondral Repair-A New Frontier for Developmental Engineering. Front Bioeng Biotechnol. 2018;6:58. [PubMed: 29868574]
9. Trindade R, Albrektsson T, Galli S, Prgomet Z, Tengvall P, Wennerberg A. Bone immune response to materials, part I: Titanium, PEEK and copper in comparison to sham at 10 days in rabbit tibia. Journal of clinical medicine. 2018;7(12):526.
10. Murray PJ, Wynn TA. Protective and pathogenic functions of macrophage subsets. Nat Rev Immunol. 2011;11(11):723–37. [PubMed: 21997792]
11. Mosser DM, Edwards JP. Exploring the full spectrum of macrophage activation. Nat Rev Immunol. 2008;8(12):958–69. [PubMed: 19029990]
12. Eijkelenboom A, Burgering BM. FOXOs: signalling integrators for homeostasis maintenance. Nat Rev Mol Cell Biol. 2013;14(2):83–97. [PubMed: 23325358]
13. Siqueira MF, Flowers S, Bhattacharya R, Faibish D, Behl Y, Kotton DN,et al. FOXO1 Modulates Osteoblast Differentiation. Bone. 2011;48(5):1043–51. [PubMed: 21281751]
14. Iyer S, Ambrogini E, Bartell SM, Han L, Roberson PK, de Cabo R, et al. FOXOs attenuate bone formation by suppressing Wnt signaling. J Clin Invest. 2013;123(8):3409–19. [PubMed: 23867625]
15. Iyer S, Han L, Bartell SM, Kim HN, Gubrij I, de Cabo R, et al. Sirtuin1 (Sirt1) promotes cortical bone formation by preventing beta-catenin sequestration by FoxO transcription factors in osteoblast progenitors. J Biol Chem. 2014;289(35):24069–78.
16. Matsuzaki T, Alvarez-Garcia O, Mokuda S, Nagira K, Olmer M, Gamini R, et al. FoxO transcription factors modulate autophagy and proteoglycan 4 in cartilage homeostasis and osteoarthritis. Sci Transl Med. 2018;10(428).
17. Jiao H, Xiao E, Graves DT. Diabetes and Its Effect on Bone and Fracture Healing. Curr Osteoporos Rep. 2015;13(5):327–35. [PubMed: 26254939]
18. Alharbi MA, Zhang C, Lu C, Milovanova TN, Yi L, Ryu JD, et al. FOXO1 Deletion Reverses the Effect of Diabetic-Induced Impaired Fracture Healing. Diabetes. 2018;67(12):2682–94. [PubMed: 30279162]
19. Lu Y, Alharbi M, Zhang C, O'Connor JP, Graves DT. Deletion of FOXO1 in chondrocytes rescues the effect of diabetes on mechanical strength in fracture healing. Bone. 2019;123:159–67. [PubMed: 30904630]
20. Kayal RA, Siqueira M, Alblowi J, McLean J, Krothapalli N, Faibish D, et al. TNF-alpha mediates diabetes-enhanced chondrocyte apoptosis during fracture healing and stimulates chondrocyte apoptosis through FOXO1. J Bone Miner Res. 2010;25(7):1604–15. [PubMed: 20200974]
21. Alblowi J, Kayal RA, Siqueira M, McKenzie E, Krothapalli N, McLean J, et al. High levels of tumor necrosis factor-alpha contribute to accelerated loss of cartilage in diabetic fracture healing. Am J Pathol. 2009;175(4):1574–85. [PubMed: 19745063]
22. Gerstenfeld LC, Wronski TJ, Hollinger JO, Einhorn TA. Application of histomorphometric methods to the study of bone repair. J Bone Miner Res. 2005;20(10):1715–22. [PubMed: 16160729]
23. Paglia DN, Diaz-Hernandez ME, Roberts JL, Kalinowski J, Lorenzo J, Drissi H. Deletion of Runx1 in osteoclasts impairs murine fracture healing through progressive woven bone loss and delayed cartilage remodeling. Journal of Orthopaedic Research®. 2020;38(5):1007–15. [PubMed: 31769548]
24. Mirando AJ, Dong Y, Kim J, Hilton MJ. Isolation and culture of murine primary chondrocytes. Methods Mol Biol. 2014;1130:267–77. [PubMed: 24482180]
25. Ma X, Su P, Yin C, Lin X, Wang X, Gao Y, et al. The Roles of FoxO Transcription Factors in Regulation of Bone Cells Function. Int J Mol Sci. 2020;21(3).

26. Gerstenfeld LC, Alkhiary YM, Krall EA, Nicholls FH, Stapleton SN, Fitch JL, et al. Three-dimensional reconstruction of fracture callus morphogenesis. J Histochem Cytochem. 2006;54(11):1215–28. [PubMed: 16864894]
27. Qin G, Zhou Y, Guo F, Ren L, Wu L, Zhang Y, et al. Overexpression of the FoxO1 ameliorates mesangial cell dysfunction in male diabetic rats Mol Endocrinol., 29 (7) (2015), pp. 1080–1091 [PubMed: 26029993]
28. Liu J, Feng X, Tian Y, Wang K, Gao F, Yang L, et al. Knockdown of TRIM27 expression suppresses the dysfunction of mesangial cells in lupus nephritis by FoxO1 pathway. J Cell Physiol. 2019;234(7):11555–66. [PubMed: 30648253]
29. Wang S, Wen X, Han XR, Wang YJ, Shen M, Fan SH, et al. Repression of microRNA-382 inhibits glomerular mesangial cell proliferation and extracellular matrix accumulation via FoxO1 in mice with diabetic nephropathy. Cell Prolif. 2018;51(5):e12462.
30. Gan L, Liu P, Lu H, Chen S, Yang J, McCarthy JB, et al. Cyclin D1 promotes anchorage-independent cell survival by inhibiting FOXO-mediated anoikis. Cell Death Differ. 2009;16(10):1408–17. [PubMed: 19575018]
31. Lees SJ, Childs TE, Booth FW. Age-dependent FOXO regulation of p27Kip1 expression via a conserved binding motif in rat muscle precursor cells. Am J Physiol Cell Physiol. 2008;295(5):C1238–46.
32. Jiang G, Huang C, Li J, Huang H, Wang J, Li Y, et al. Transcriptional and post-transcriptional upregulation of p27 mediates growth inhibition of isorhapontigenin (ISO) on human bladder cancer cells. Carcinogenesis. 2018;39(3):482–92. [PubMed: 29409027]
33. Kurakazu I, Akasaki Y, Hayashida M, Tsushima H, Goto N, Sueishi T, et al. FOXO1 transcription factor regulates chondrogenic differentiation through transforming growth factor beta1 signaling. J Biol Chem. 2019;294(46):17555–69.
34. McDonald MM, Morse A, Mikulec K, Peacock L, Baldock PA, Kostenuik PJ, et al. Matrix metalloproteinase-driven endochondral fracture union proceeds independently of osteoclast activity. J Bone Miner Res. 2013;28(7):1550–60. [PubMed: 23408642]
35. McDonald MM, Morse A, Peacock L, Mikulec K, Schindeler A, Little DG. Characterization of the bone phenotype and fracture repair in osteopetrotic incisors absent rats. J Orthop Res. 2011;29(5):726–33. [PubMed: 21437952]
36. Guerne PA, Carson DA, Lotz M. IL-6 production by human articular chondrocytes. Modulation of its synthesis by cytokines, growth factors, and hormones in vitro. J Immunol. 1990;144(2):499–505. [PubMed: 2104896]
37. Axmann R, Bohm C, Kronke G, Zwerina J, Smolen J, Schett G. Inhibition of interleukin-6 receptor directly blocks osteoclast formation in vitro and in vivo. Arthritis Rheum. 2009;60(9):2747–56. [PubMed: 19714627]
38. Tamura T, Udagawa N, Takahashi N, Miyaura C, Tanaka S, Yamada Y, et al. Soluble interleukin-6 receptor triggers osteoclast formation by interleukin 6. Proc Natl Acad Sci U S A. 1993;90(24):11924–8.
39. Jiménez-García L, Herranz S, Higueras MA, Luque A, Hortelano S. Tumor suppressor ARF regulates tissue microenvironment and tumor growth through modulation of macrophage polarization. Oncotarget. 2016;7(41):66835.
40. Wu X, Xu W, Feng X, He Y, Liu X, Gao Y, et al. TNF-a mediated inflammatory macrophage polarization contributes to the pathogenesis of steroid-induced osteonecrosis in mice. Int J Immunopathol Pharmacol. 2015;28(3):351–61. [PubMed: 26197804]
41. Viniegra A, Goldberg H, Cil C, Fine N, Sheikh Z, Galli M, et al. Resolving Macrophages Counter Osteolysis by Anabolic Actions on Bone Cells. J Dent Res. 2018;97(10):1160–9. [PubMed: 29993312]
42. Klinkert K, Whelan D, Clover AJP, Leblond AL, Kumar AHS, Caplice NM. Selective M2 Macrophage Depletion Leads to Prolonged Inflammation in Surgical Wounds. Eur Surg Res. 2017;58(3–4):109–20. [PubMed: 28056458]
43. Orecchioni M, Ghosheh Y, Pramod AB, Ley K. Macrophage Polarization: Different Gene Signatures in M1(LPS+) vs. Classically and M2(LPS−) vs. Alternatively Activated Macrophages. Front Immunol. 2019;10:1084. [PubMed: 31178859]

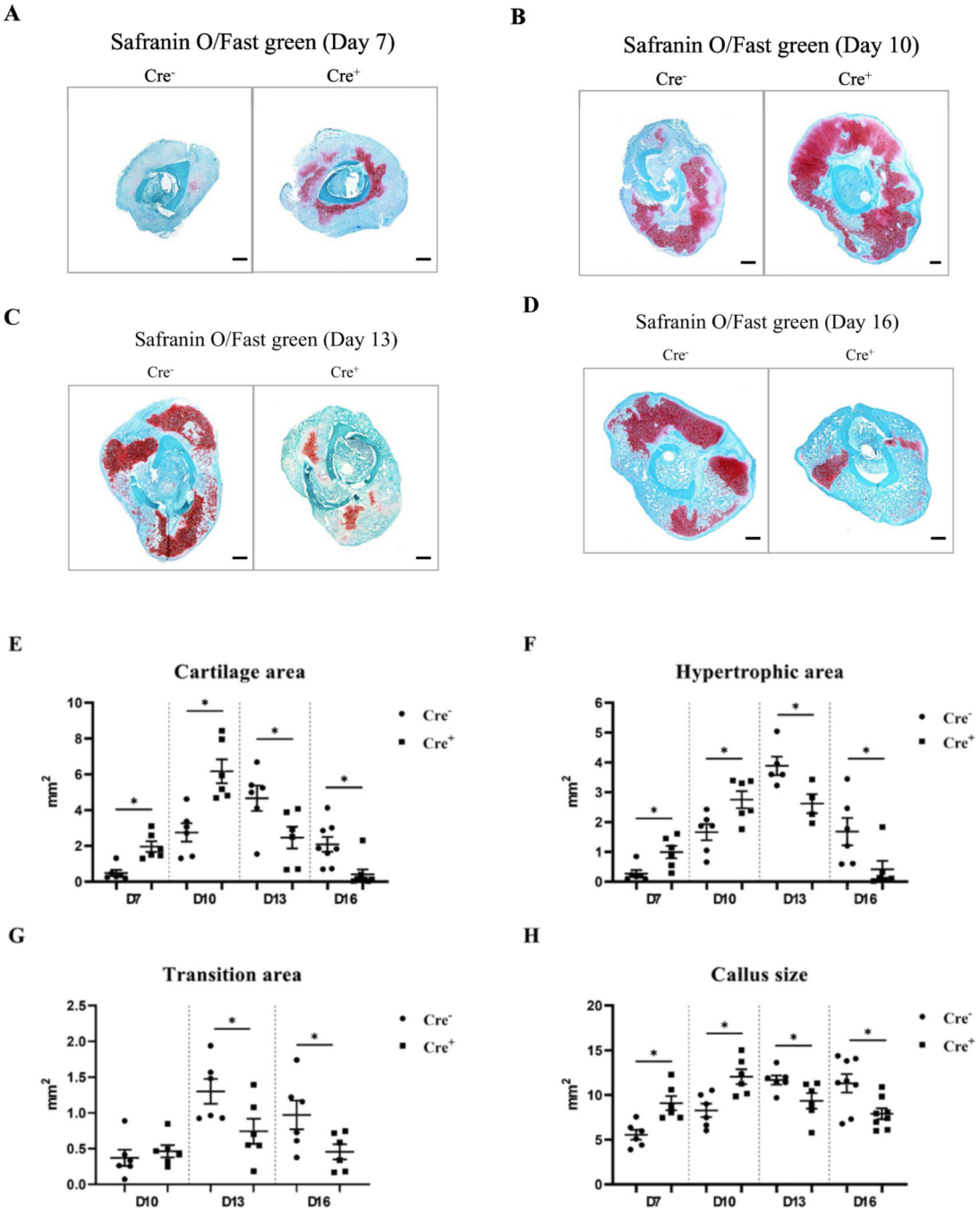

Fig. 1.

FOXO1 deletion in chondrocytes increases both cartilage formation and loss. Safranin O/fast green histostaining was performed on sections from Col2α1Cre^{-}FOXO1$^{L/L}$ and Col2α1Cre^{+}FOXO1$^{L/L}$ mice on days 7, 10, 13 and 16 after the fracture. Histomorphometric analysis was carried out with computer-assisted image analysis. (A-D) Representative images that show the entire samples are composed of 4x images. Scale bars = 300 μm. (E) Cartilage area. (F) Areas of hypertrophic chondrocytes. (G) Area of the transition zone (chondro-osseous junction). (H) Callus area. Data are presented as the mean ± SE. * $p < 0.05$, n = 5–7

mice in each group. Cre^{-} = Col2α1Cre^{-}FOXO1$^{L/L}$; Cre^{+} = Col2α1Cre^{+}FOXO1$^{L/L}$; D = days.

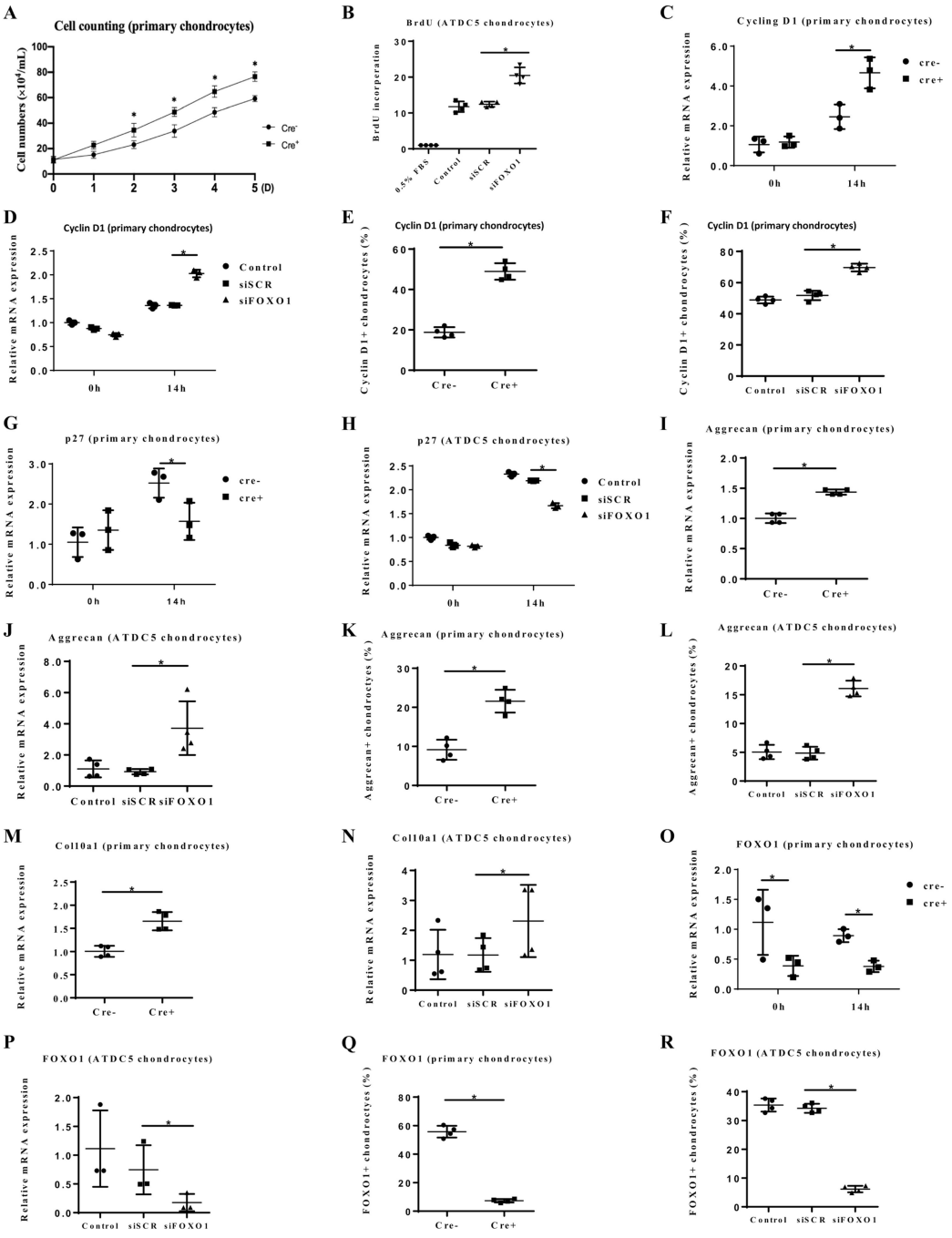

Fig. 2.

FOXO1 deletion in chondrocytes promotes cell proliferation and the expression of cartilage matrix genes. (A) Primary chondrocytes were obtained from Col2α1Cre^{-}FOXO1$^{L/L}$ and Col2α1Cre^{+}FOXO1$^{L/L}$ mice and cultured in 5% FBS. The number of chondrocytes was counted at the indicated time points. (B) BrdU assay was performed with ATDC5 chondrocytes transfected with scrambled siRNA, FOXO1 specific siRNA or no transfection. Cells were incubated with or without 10% FBS. (C, D) Chondrocytes were stimulated by 10% FBS and Cyclin D1 was measured by RT-PCR 14h later in primary chondrocytes from

experimental and control mice or ATDC5 chondrocytes without or with siRNA transfection as indicated. (E, F) Cyclin D1 was measured by flow cytometry in primary chondrocytes and ATDC5 chondrocytes as described in panels C and D. (G, H) p27 expression was measured in primary chondrocytes from experimental or control mice or in ATDC5 chondrocytes with RNAi as described above. (I-L) The expression of Aggrecan protein core was measured in primary chondrocytes from experimental or control mice and ATDC5 chondrocytes with FOXO1 knockdown by RNAi as described above. (M, N) Col10α1 mRNA levels were measured in primary chondrocytes from experimental or control mice and ATDC5 chondrocytes with FOXO1 knockdown by RNAi. (O-R) The expression of FOXO1 in primary chondrocytes from experimental or control mice or ATDC5 chondrocytes with FOXO1 knockdown by RNAi was tested by RT-PCR or flow cytometry as described above. Data are presented as the mean ± SE, * $p < 0.05$, n = 5–7 mice in each group. Cre^{-} = $Col2\alpha1Cre^{-}FOXO1^{L/L}$; Cre^{+} = $Col2\alpha1Cre^{+}FOXO1^{L/L}$; D = days; h = hours; siSCR = scrambled siRNA; siFOXO1 = FOXO1 siRNA.

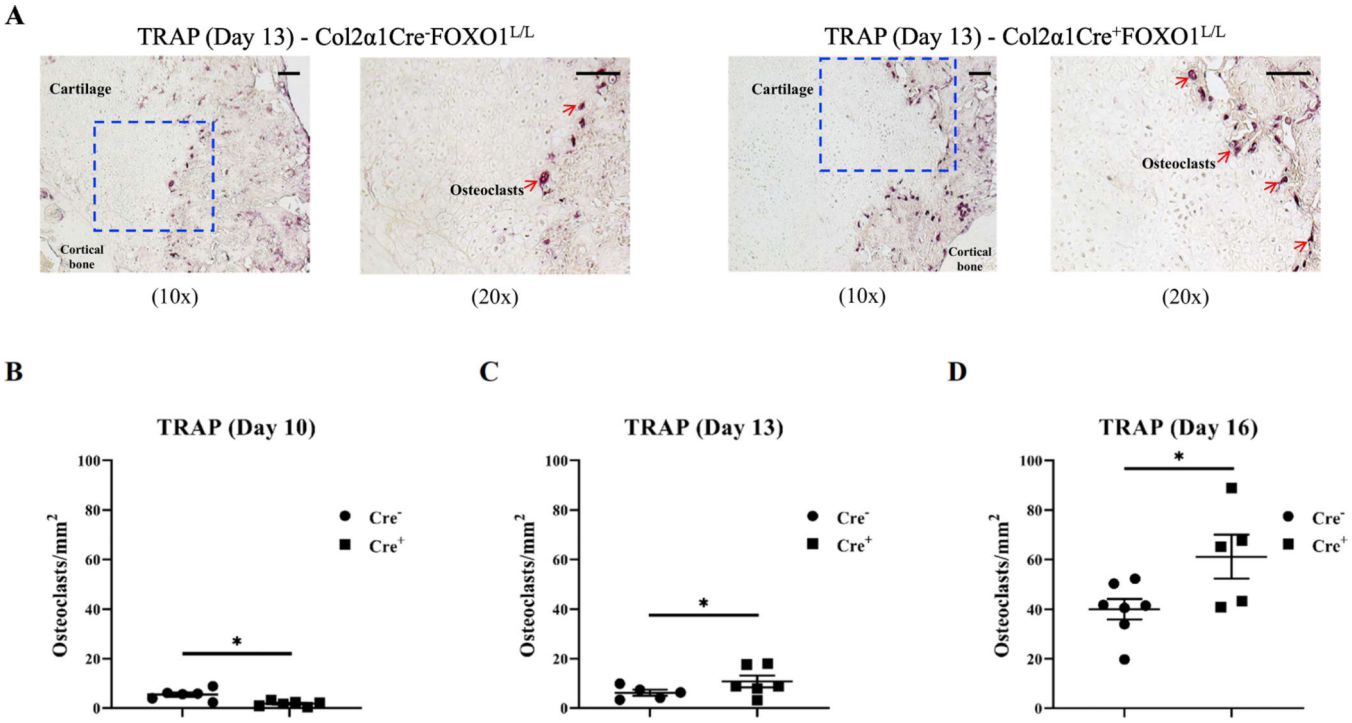

Fig. 3.

FOXO1 deletion in chondrocytes increases osteoclast numbers. TRAP staining was performed on sections from experimental and control mice to evaluate the number of cartilage-lining osteoclasts. (A) Representative images of Col2α1Cre^{-}FOXO1$^{L/L}$ and Col2α1Cre^{+}FOXO1$^{L/L}$ mice. The magnification of the low power is 10x and the high power is 20x. Scale bars = 100 μm. (B-D) The number of osteoclasts was measured per cartilage area in sections from Col2α1Cre^{-}FOXO1$^{L/L}$ and Col2α1Cre^{+}FOXO1$^{L/L}$ mice on days 10, 13 and 16 after fracture. Data are presented as mean ± SE, * $p < 0.05$, n = 5–7 mice in each group. Cre^{-} = Col2α1Cre^{-}FOXO1$^{L/L}$; Cre^{+} = Col2α1Cre^{+}FOXO1$^{L/L}$.

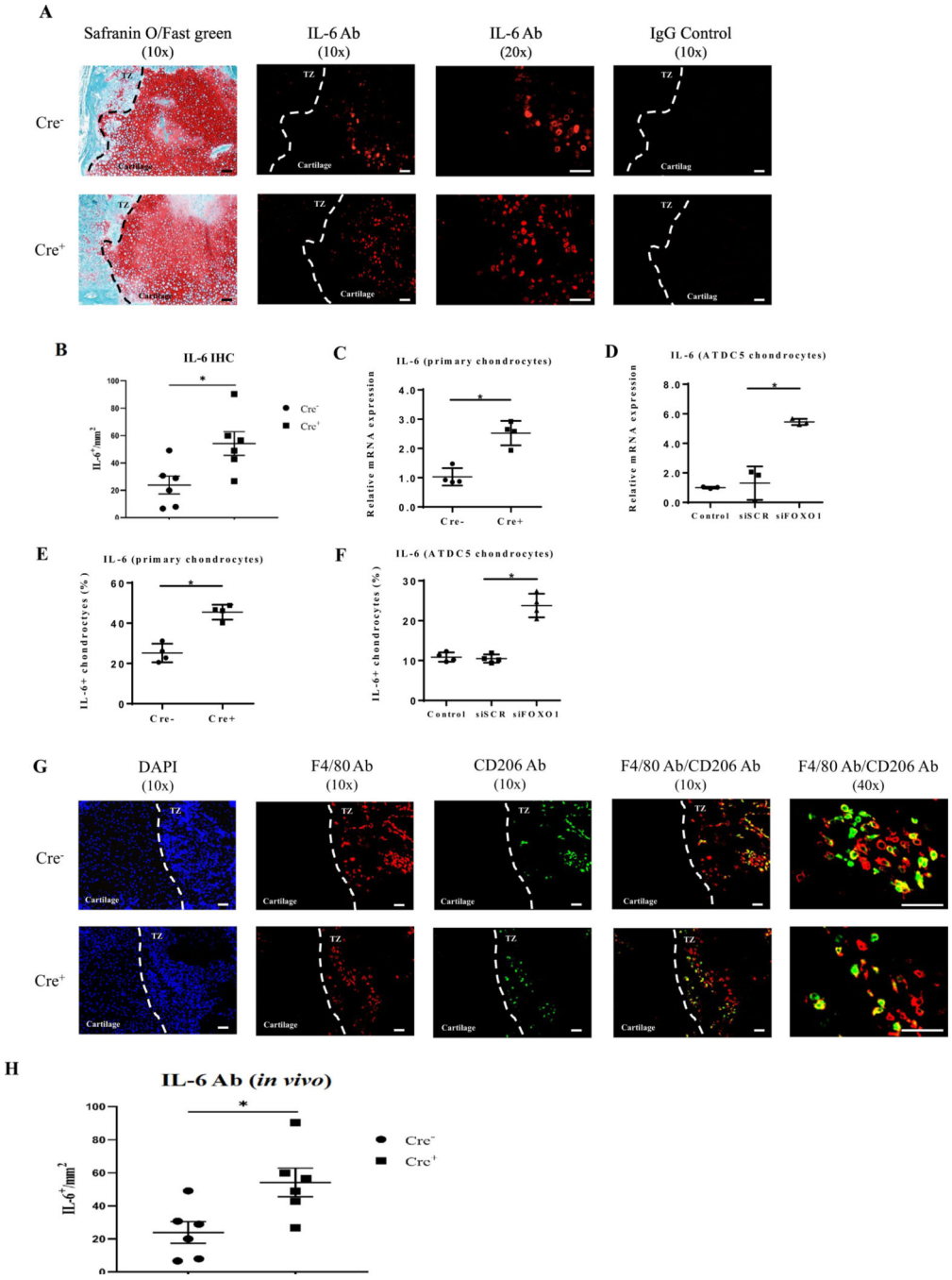

Fig. 4.

FOXO1 regulates IL-6 expression and the formation of M2-like macrophages. IL-6 was measured by immunofluorescence as IL-6^{+} immunopositive cells using a specific antibody for antigen. Matched control antibody was negative. Representative immunofluorescence images of sections obtained from Col2α1Cre^{-}FOXO1$^{L/L}$ and Col2α1Cre^{+}FOXO1$^{L/L}$ mice 13 days after fracture are shown in comparison with adjacent sections stained with Safranin O/Fast green. The magnification of the low power is 10x and the high power is 20x. Scale bars = 100 μm. (B) The number of IL-6 immunopositive chondrocytes was measured in

paraffin histologic sections described above. (C-F) The expression of IL-6 was measured in vitro in primary chondrocytes from experimental and control mice and in ATDC5 chondrocytes with FOXO1 knockdown by RNA by RT-PCR or by flow cytometry. (G) M2-like macrophages were detected by immunofluorescence. Histologic sections show $F4/80^{+}$ (green), $CD206^{+}$ (red) and double $F4/80^{+}/CD206^{+}$ (yellow) cells at low power is 10x and high power 40x images. Scale bars = 100 μm. (H) The number of F4/80 and CD206 double immunopositive cells in the area of the transition zone were measured in sections described above. Data are presented as mean ± SE, * $p < 0.05$, n = 5–7 mice in each group. Ab = antibody; Cre^{-} = $Col2\alpha1Cre^{-}FOXO1^{L/L}$; Cre^{+} = $Col2\alpha1Cre^{+}FOXO1^{L/L}$; TZ = transition zone; siSCR = scrambled siRNA; siFOXO1 = FOXO1 siRNA.

Table 1.

Bone volume and total callus volume on day 16 and 22 Measured by Micro-CT

FOXO1 deletion in chondrocytes alters bone formation during fracture healing, Micro-CT was performed on fracture calluses on 16 and 22 days after fracture in Col2a1Cre^{-}.FOXO1$^{L/L}$ mice and Col2a1Cre^{+}.FOXO1$^{L/L}$ mice. n = 6–8/group and data represent the mean with standard deviation in parentheses.

	Cre^{-}	Cre^{+}	*P*-value (Cre^{-} vs Cre^{+})
D16 Bone Volume (mm^3)	32.82 (3.88)	28.27 (2.1)	0.03
D16 Total Callus Volume (mm^3)	65.21 (7.8)	53.38 (4.24)	0.007
D16 Bone Volume/Total Volume	0.5 (0.03)	0.53 (0.048)	0.26
D22 Bone Volume	24.32 (3.9)	17.07 (4.8)	0.006
D22 Total Callus Volume (mm^3)	46.96 (8.5)	31.37 (7.7)	0.003
D22 Bone Volume/total Volume (mm^3)	0.52 (0.58)	0.55 (0.07)	0.48